

# TEG Heat Sink Dynamic Surface Temperature Measurement Utilizing Thermographic Phosphor

Seongmin Kang<sup>a</sup>, Myungjin Seo<sup>a</sup>, Kyungjun Lee<sup>a</sup>, Mori Hideo<sup>b\*</sup>, Jae-Ho Jeong<sup>a\*\*</sup>

<sup>a</sup>Department of Mechanical Engineering, Gachon University, Gyeonggi-do, 13120, Republic of Korea

<sup>b</sup>Department of Mechanical Engineering, Kyushu University, 744 Motoooka, Nishi-ku, Fukuoka, 819-0395, Japan

\*Corresponding author: [hide-m@mech.kyushu-u.ac.jp](mailto:hide-m@mech.kyushu-u.ac.jp)

\*\*Corresponding author: [Jaeho.jeong@gachon.ac.kr](mailto:Jaeho.jeong@gachon.ac.kr)

\***Keywords** : TEG (Thermoelectric Generator), Thermographic phosphor, CFD Analysis, Heat Exchange, Heat Sink

## 1. Introduction

Thermoelectric generator (TEG) is a renewable energy production method that exchanges wasted thermal energy, typically from high-temperature heat sources, for electrical energy. TEG plays an important role in sustainable energy production and waste heat recovery. The technology is utilized in a variety of applications, but it can be applied very effectively to generate electricity by utilizing waste heat from large mechanical systems, such as nuclear power plant. nuclear power plant operates under high temperature conditions, which results in a significant amount of thermal energy being dissipated or wasted. It is known as about 33% of the thermal energy produced in nuclear reactions is converted into electricity, the remaining 67 is released, for example, into the sea, etc, as waste heat [1]. However, efficiently recovering this thermal energy and converting it into electrical energy is an environmentally friendly and economical solution. Integrating TEG within nuclear reactors can not only recover the high-temperature thermal energy generated within the reactor core, but also improve the resilience and safety of nuclear power plants by allowing the TEG system to provide emergency power by utilizing the thermal energy generated in the core in the event of a nuclear accident or overload operation.

The role of a heat sink in a TEG system is to dissipate thermal energy from a hot heat source to a cooler side. A heat sink is connected to a TEG device to facilitate heat transfer and improve thermal conductivity. This enables efficient transfer of thermal energy generated by the TEG and maximum electrical output. Therefore, it is important to design and evaluate heat sinks with high heat exchange performance.

To evaluate the heat exchange performance of a designed heat sink, it is necessary to measure the temperature gradient of the heat sink where heat exchange occurs. Currently, there are various techniques available to measure the temperature. There are invasive methods such as contacting thermocouples, etc. and non-invasive methods like infrared cameras, pyrometer, etc [2]. In this study, we chose to use a thermographic phosphor for measuring the temperature gradient of the heat exchange fins.

Thermographic phosphors are a type of phosphor that exhibit different luminescence responses depending on temperature. The luminescence of a thermographic phosphor is a function of local temperature, so each pixel in the image captured by the camera acts as a thermocouple. The most well-known responses that can be used for temperature measurement are emission lifetime and emission intensity. By measuring the luminescence properties of the luminescent particles to be used in the experiment, suitable measurement method can be chosen for the experiment's purpose.

In this study, an experimental device was designed to evaluate the heat exchange performance of a thermoelectric fin designed using thermographic phosphor. CFD analysis was used to verify the feasibility of the experimental device. We have built a wind tunnel chamber and will be using a thermographic phosphor to evaluate the performance of a heat exchange with constant flow rates. We want to compare the temperature distribution measured by thermographic phosphor with the temperature distribution measured by thermal imaging camera and match the results with CFD analysis result.

## 2. Methods and Results

### 2.1 Thermographic Phosphor

The thermographic phosphor used in this study was BAM:EuMn (TOKYO KAGAKU KENKYUSHO CO., LTD.) with an average particle size of approximately 8  $\mu\text{m}$ , shown in Fig. 1. BAM:EuMn (aka. BAM:G,  $\text{BaMgAl}_{10}\text{O}_{17}:\text{EuMn}$ ) is the Modification of the dopant material from the existing blue Phosphor, BAM:Eu ( $\text{BaMg}_2\text{Al}_{10}\text{O}_{17}:\text{Eu}$ ) Phosphor. While the Base phosphor BAM:Eu has several research data, there are rarely research reports or data for the dopant-modified BAM:EuMn that will be used in this study.

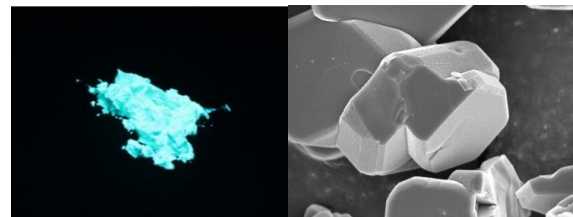


Fig. 1. BAM:G Phosphor powder.

## 2.2 Preparing Paint and Surface coating

To measure the thermo-luminescence properties of this BAM:G phosphor, a copper specimen (45 mm × 45 mm × 0.5 mm) was sprayed with a mixture of BAM:G phosphor and ceramic binder (ZYP BNSL Binder, Oak Ridge, USA) using a dual-function airbrush (Iwata G3) with adjustable air and liquid flow to create a coating. The best results were obtained when the ratio of phosphor, binder, and diluent (ethanol) was 1 g:0.6 ml:4.4 ml, respectively. This mixture was placed in a beaker and carefully mixed with a glass rod until it became a relatively viscous liquid, which was sprayed evenly onto the substrate using an airbrush, shown in Fig. 2. In Fig. 3, The painted sample shows blue-green emission luminescence under UV excitation light.



Fig. 2. BAM:G Phosphor paint mixing and spraying process

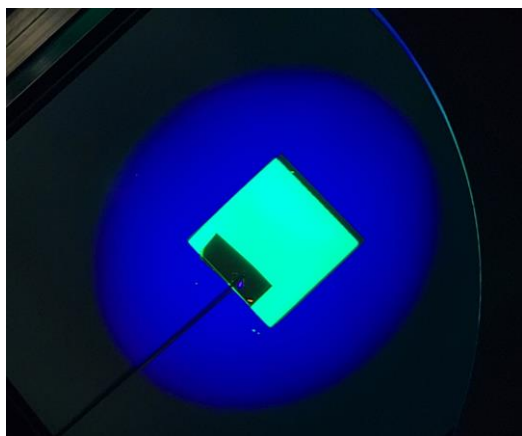


Fig. 3. BAM:G Phosphor paint specimen luminescence under UV excitation light

## 2.3 Calibration Chamber design

To determine temperature using thermographic phosphor paint, a calibration process is essential. To achieve this, the specimen is heated to specific temperatures, and images are captured to establish a correlation between the observed luminescence and the corresponding temperature values. For the calibration of the thermographic phosphor using in this study, a calibration chamber was designed. In order to determine the transfer function between the recorded luminescence properties and the surface temperature, a device that maintains a constant and uniform temperature of the test sample over an extended period

of time is required. The schematic of designed calibration chamber is shown in Fig. 4.

Aluminum profiles were assembled to form the chamber structure, and aluminum plates were used to form and seal the chamber walls. The hot plate was placed inside the chamber to heat the specimen. The temperature of the hot plate and the specimen are measured simultaneously using K-type sheath thermocouples. For this calibration chamber, an illuminator was designed to be mounted outside the chamber to illuminate the specimen inside the chamber. In addition, an ultra-high-speed camera was used to measure the luminescence lifetime characteristics of the phosphor. To allow the UV light from the illuminator to reach the inside of the chamber, fused silica glass with high UV transmission properties was mounted on the top of the chamber. The ultra-fast camera used in this chamber was a Photron Fastcam mini AX50, and the UV illuminator was a HARDsoft IL-106X Illuminator.

Calibration is accomplished by utilizing the PID control of the hot plate to uniformly heat the specimen to a constant temperature. A thermographic phosphor sample heated on a hot plate at a constant temperature for a sufficiently long time is warmed up to its thermal equilibrium temperature. Then properly excite the phosphor specimen utilizing illuminator with phosphor's excitation wavelength, and then measure the luminescence properties exhibited by the luminescent as a function of specimen temperature. In this study, temperature measurements were performed using the intensity method, which measures the luminescence intensity of the phosphor.

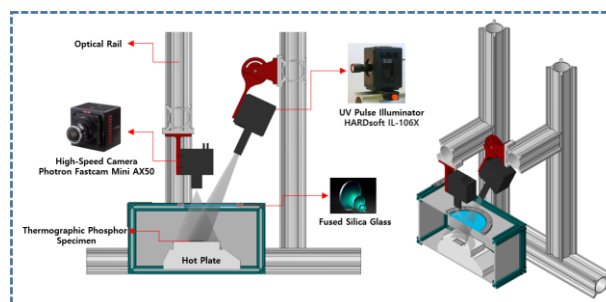


Fig. 4. Schematic of the thermographic phosphor calibration chamber

## 2.4 Calibration

The calibration was performed simultaneously on a copper plate specimen and a heat sink specimen, shown in Fig. 5. Both specimens were painted using equal paint formulations and annealed at 250°C for 24 hours to complete the film. The specimens were placed on a hot plate, and a K-type thermocouple was attached to the copper plate specimen to measure the actual surface temperature. The specimen was heated from 20 to 250°C, and the UV LED was activated to record the luminescence of the specimen when it reached thermal equilibrium at each measurement temperature. The

temperature-dependent luminescence intensity was measured by the camera was analyzed using MATLAB.

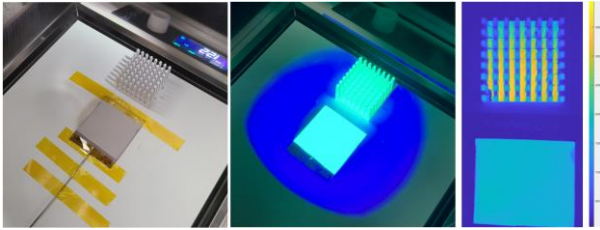


Fig. 5. BAM:G phosphor calibration process

The calibration result is shown in Fig. 6. Both copper plate specimen and a heat sink specimen exhibited the same temperature-luminescence intensity characteristics. The calibration showed that the intensity ratio increased from 20 to 50°C and then decreased again. This suggests that temperature measurements are possible around 200°C, which is the temperature region of interest for this experiment. Temperature measurement of an actual heat sink can be done by measuring the luminescence intensity of the heat transfer fin at a specific reference temperature, and then measuring the intensity in a heat exchange environment, the intensity ratio is then calculated and compared to this calibration curve.

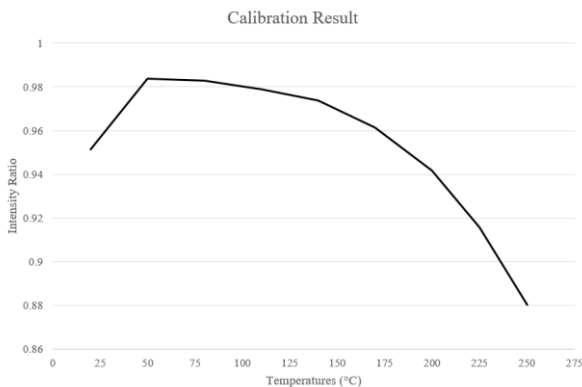


Fig. 6. BAM:G phosphor calibration result

### 2.5 Dynamic Temperature Measurement

In order to measure the change in luminescence intensity as the temperature of the specimen changes, the copper plate specimen was cooled using a portable air blower. While the specimen was kept at a constant 250 degrees, a spray type air blower was applied for 1 second and the change in luminescence intensity was recorded. The resulting time - luminescence intensity ratio graph is shown in the Figure below. At 45.32s, the air blower was injected, and at approximately 46.5s, the injection ended. During the approximately 1 second of injection, we observed that the intensity ratio increased from 0.881 to 0.9077, and after matching with the calibration curve, we found that the average temperature of the specimen decreased from 249.5°C to

230.62°C. At 47s, after the blowing ended, the temperature of the sample had recovered to 242.5°C.

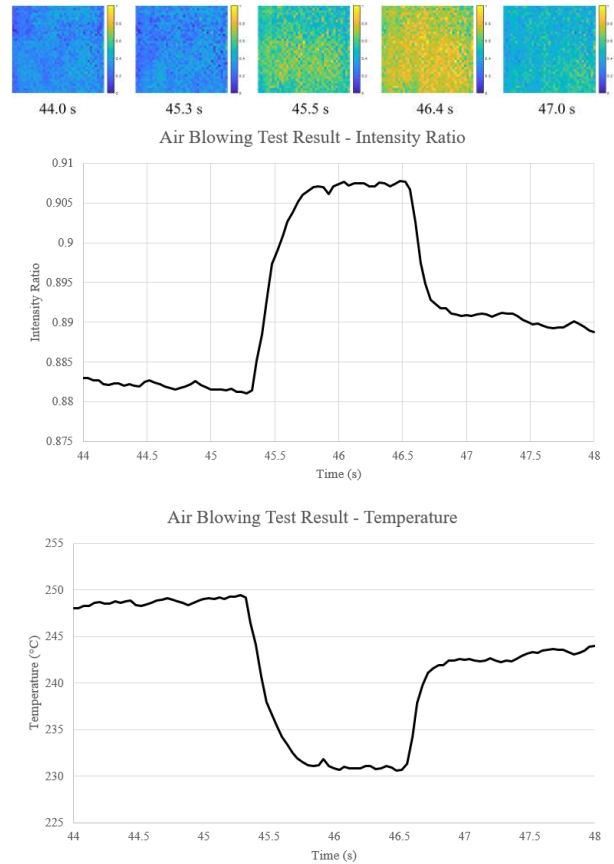


Fig. 7. BAM:G phosphor dynamic temperature measurement result

### 2.6 Test Facility Design

A schematic of the experimental apparatus for evaluating the heat exchange performance of a thermoelectric generator fin utilizing thermographic phosphor is shown in Fig. 8.

The components of designed experimental facility are listed in Table I. The apparatus has the structure of a wind tunnel. At the end of the tunnel, an air blower generates the flow inside the wind tunnel chamber. A heating plate is installed inside the chamber to heat the specimen. The heat exchange fin specimen will be coated with thermographic phosphor paint. To measure the responses emitted by the thermographic phosphor paint, a CMOS camera is installed vertically on the top of the heating plate and photographed. The luminescence properties of the thermographic phosphor specimen in the resulting images are subjected to image analysis to measure the temperature distribution of the specimen. To ensure constant measuring conditions, LED lights are installed around the CMOS camera to maintain constant photographing conditions. For flow rate and velocity, PIV measurement will be performed.

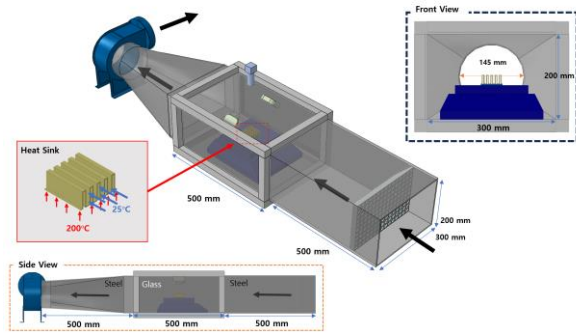


Fig. 8. 3D modeling of the TEG heat exchange wind tunnel test bench.

Table I: TEG heat exchange test bench components

No.	Function	Component	Features
1	Hot Plate	ASONE NDK-1A-F	Max. Temperature 350°C
2	IR Camera	HIKMICRO Pocket2	256 x 192 -20°C to 400°C
3	CMOS Camera	Basler ace acA1920-25uc	1,920 x 1,080 25 fps
4	LED Light	Ulanzi L2 Cute Lite	1000LUX (0.5m), 300LUX (1.0m)
5	Thermo couple	MISUMI SSMJ1-50	Max. Temperature 450°C
6	Air Blower	DongKun Industrial DB-10C-1	Air Mass Flow Rate 0.1 kg/s

## 2.7 CFD Analysis

CFD analysis was performed to verify the design specifications of the experimental equipment. Using CAD modeling of the wind tunnel chamber, preliminary verification was performed by calculating the same analysis conditions as the actual experimental conditions.

The geometric information of the randomly designed heat sink is shown in Table II and Fig. 9. The heat transfer fins have an overall size of 50mm \* 50mm \* 20mm and are assumed to be made of copper. There is a 50mm \* 50mm \* 3mm plate between the heat sink and the heat exchange fins. High-temperature air was passed through the experimental equipment using a test blower. The grid consists of approximately 10 million elements, and analysis was conducted using the commercial software Ansys CFX to perform thermal analysis of the experimental setup.

Table II: Heat sink geometry parameters

Heat Sink Parameters	Dimensions (mm)
Fins height, H	20
Thickness, T	1
Length of heat sink, L	50
Width of heat sink, W	50
Fins Thickness, S1	10
Fin Spacing, S2	10

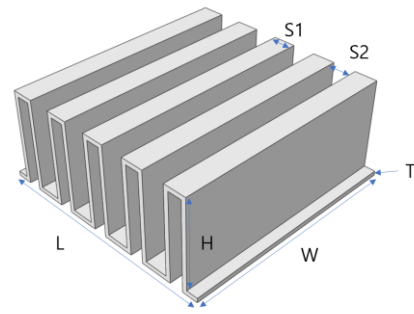


Fig. 9. Heat sink geometry parameters.

The boundary conditions applied for the CFD analysis have been shown in Table III. The air inlet was configured as a pressure inlet, and the turbulence model employed was the SST model. The air inlet mirrored the experimental setup, maintaining a mass flow rate of 0.1 kg/s, with ambient air at 25°C and standard pressure flowing uniformly through a 300mm x 200mm chamber. It was assumed that the base of the heat sink remained at a constant temperature of 200°C, allowing for unrestricted heat exchange with the heat transfer Fins.

Table III: Boundary condition for CFD

Domain	Parameter	Value [unit]
Air	Inlet Temperature	25 [°C]
	Pressure Inlet	1 [atm]
	Velocity outlet	0.1[kg/s]
	Turbulence Model	SST
Fin	Material	Copper
Hot plate	Temperature	200 [°C]

The CFD analysis focused on the internal components of the experimental equipment, specifically the hot plate and the heat transfer Fin.

The temperature distribution for the heat transfer Fin is shown in Fig. 10. For the heat transfer Fins, the temperature distribution at the leading edge where they first come into contact with the ambient air was 188.6°C. At the top portion of the hot plate, a temperature distribution of 189.2°C was observed, while the maximum temperature at the bottom surface of the hot plate reached 190.02°C. This result suggesting that the temperature gradient on the paint during the thermographic phosphor experiment is expected to be low.

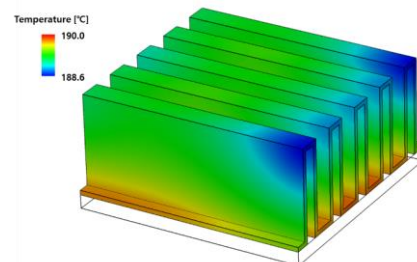


Fig. 10. Distribution of Fin temperature.

In this study, CFD analysis was conducted with the hot plate temperature set above 200°C to replicate conditions similar to waste heat in nuclear power plant application. To assess the validity of the actual experimental equipment, additional CFD analyses are being carried out under various conditions, where the hot plate temperature and the ambient air velocity are varied.

These CFD analysis results, in conjunction with comparisons to the actual experimental apparatus, will serve as a means to validate the suitability of the experimental setup.

### **3. Conclusions**

In this study, we designed an experimental setup for surface temperature measurement using BAM:G thermographic phosphor. We confirmed that surface temperature measurement is possible even in the high temperature region above 200°C. Dynamic temperature measurements using an air blower were performed to confirm high-temperature surface thermometry is possible with high spatial and temporal resolution. A wind tunnel chamber was designed and fabricated to measure the heat exchange performance of a real heat transfer fin. CFD analysis was performed to measure the temperature gradient of the heat transfer fin to validate the experimental setup. In a follow-up study, the thermographic phosphor will be applied to a real developed TEG heat sink to evaluate the heat exchange performance under controlled conditions.

### **Acknowledgment**

This work was supported by Korea Institute of Energy Technology Evaluation and Planning (KETEP) grant funded by the Korea government (MOTIE)(RS-2023-00243201, Global Talent Development project for Advanced SMR Core Computational Analysis Technology Development), JSPS KAKENHI Grant Number JP23K03661 and Harada Memorial Foundation.

### **REFERENCES**

- [1] Obara, S. Y., & Tanaka, R. (2021). Waste heat recovery system for nuclear power plants using the gas hydrate heat cycle. *Applied Energy*, 292, 116667.
- [2] Burner, A.W.; Liu, T.; Garg, S.; Bell, J.H.; Morgan, D.G. Unified Model Deformation and Flow Transition Measurements. *J. Aircr* 1999, 36, 898–901.